Supporting Information for

In-situ growth of $WO_3/BiVO_4$ nanoflowers onto cellulose fibers to construct photoelectrochemical/colorimetric lab-on-Paper device for ultrasensitive detection of AFP

Xu Li[a], Kang Cui[a,*], Mingzhen Xiu[b], Chenxi Zhou[a], Li Li[a,], Jing Zhang[a], Shiji Hao[c], Lina Zhang[d], Shenguang Ge[a], Yizhong Huang[b,*], Jinghua Yu[a,*]

[a] *School of Chemistry and Chemical Engineering, University of Jinan, Jinan 250022, PR China*

[b] *School of Materials Science and Engineering, Nanyang Technological University, Singapore 639798, Singapore*

[c] *School of Materials Science & Engineering, Dongguan University of Technology, Guangdong 523808, PR China*

[d] *Shandong Provincial Key Laboratory of Preparation and Measurement of Building Materials, University of Jinan, Jinan, 250022, PR China*

* Corresponding authors.

E-mail addresses: chm_cuik@ujn.edu.cn (K. Cui), yzhuang@ntu.edu.sg (Y. Huang), ujn.yujh@gmail.com (J. Yu).

Contents

Preparation of Au-PWE

According to the previous literatures, the Au nanoparticles modified paper working electrode (Au-PWE) was obtained by growing a layer of Au nanoparticles on the surface of cellulose fibers.[1] In a word, 80 ml of deionized water was put into a three-necked flask and heated to 90 ℃, then 0.8 ml of 1% $HAuCl_4$ solution was added to the above solution and heated to 96 ℃ for 1 min. Next, 2.8 ml of 1% trisodium citrate was added and stirred for 15 min. Finally, the solution was stirred and cooled to obtain a gold seed solution. Subsequently, 80 μL of hydroxylamine hydrochloride and gold seed solution (volume ratio 1:1) was dropped on the surface of working electrode each time and dried at room temperature. After repeated dripping five times, it was thoroughly washed with deionized water and dried. The Au nanoparticles modified PWE was successful preparation.

Design of the dual-mode lab-on-paper device

Inspired by the merits of paper folding, the dual-mode lab-on-paper photoelectrochemical (PEC)/colorimetric immunosensor platform was designed for detection of AFP. The pattern and size of the lab-on-paper device were designed by Adobe Illustrator CS4 (Fig. S1) and printed on Whatman No.2 chromatography paper using a wax printer. Subsequently, the wax-printed papers were baked at 150 ℃ for 60 s to make sure that the wax formed a hydrophobic zone on the paper (Fig. S2, S3). As demonstrated in Figure S1B and C, the lab-on-paper device included the PEC detection tab (green 30 mm × 35 mm), electrode tab (orange, 30 mm × 12.5 mm), colorimetric tab (30 mm × 12.5 mm) and washing tab (30 mm × 35 mm). These unprinted detection zone and auxiliary zone were used for the screen-printing of electrodes (work electrode, Ag/AgCl reference and carbon counter electrode). The lantern -shaped region with a diameter of 10 mm on the PEC detection tab was the detection region, which was used to realize the PEC detection. And the detection area could fold up so that the electrodes can be modified better in the following process, after cut by knife along the sides (Fig. S4A and B). During the electrode modification process, the detection area would be

overlapped the rest hydrophobic region of the PEC detection tab, preventing the modification fluid flowing down by gravity. After modification, the washing tab will fold down to make sure the rectangle 3 mm wide contact the detection area to lead the excess fluid flow to big rectangle (waste liquid pool) to collect the waste fluid (Fig. S4C and D).

In order to realize the PEC detection, there are two squares with 5 mm long could expose the counter electrode and reference electrode on the detection tab when the electrode tab was folded to right. The electrode tab has a circle with a diameter 10 mm, and the Ag/AgCl reference electrode and carbon counter electrode were printed on the corresponding place via screen-printing technique. By now, the lab-on-paper device could accomplish the PEC detection. After the PEC detection, the rest solution could flow to the washing tab by folding down the washing tab. The colorimetric tab with a circle (diameter 10.5 mm) which was split by a hydrophobic rectangle (2 mm×12 mm) to a color area and a check plot, and TMB was embedded in the hydrophobic during the process. To realize colorimetric detection, the color tab was folded left to cover the detection zone and added 1 mL PBS containing 200 μL of H_2O_2 (5 mM).

Assembly and operation of lab-on-paper device

A→B：To modify the working zone of PEC detection tab, the PEC detection tab is folded as shown in the Fig. 1B so that the Au NPs, $WO_3/BiVO_4$ nanoflower, and Ab can be modified on the surface of cellulose fiber.

B→C: To remove the waste liquid from the modification process, the washing tab is folded down so that the waste liquid could be removed with washing tab.

C→D: Fold the electrode tab to the right, and fold the PEC detection tab upward to make the working electrode contacting with the printed electrodes to achieve PEC detection.

D→E: The colorimetric tab is folded to the left so that the embedded TMB contacts the $WO_3/BiVO_4$ materials and H_2O_2 for realizing colorimetric detection.

The effects of WO_3/$BiVO_4$ heterojunction.

Tauc plot has been used to calculate the band gap of semiconductor and the formula is $(\alpha hv)^n = A(hv - E_g)$ (α: absorption coefficient; h: Plank's constant; v: photon's frequency; A: proportionality constant; E_g: the band gap; n: the type of the electronic transitions (for example WO_3 is indirect band gap semiconductor, the value of n is 0.5; the $BiVO_4$ is direct band gap semiconductor, the value of n is 2)).[2] Here, the band gap of WO_3, $BiVO_4$, and WO_3/$BiVO_4$ were 2.6, 2.45, 2.34, respectively, which were calculated by Tauc plot. (Fig. S6A) And the Tauc plots were clearly shown that the band gap of WO_3/$BiVO_4$ was smaller than others, which indicated the heterojunction formed by WO_3 and $BiVO_4$ was beneficial to broaden the light absorption range. Besides, as shown in Fig. S6B, the photocurrent signal of WO_3/$BiVO_4$ electrode is clearly higher than that of $BiVO_4$ electrode, indicating that the formation of WO_3/$BiVO_4$ heterojunction is conducive to the improvement of photocurrent.

Modification process of the working electrode

Briefly, first, a layer of Au NPs was grown on the surface of PWE to enhance the conductivity of fiber. Second, the WO_3/$BiVO_4$ heterojunction was modified to the surface of Au-PWE. Next, CS solution (10 μL, 0.1 wt%) was dropped to electrode surface and dried at room temperature, and washed by NaOH and DI water, respectively. Then, the GLD (25 μL, 5%) solution was dropped onto the electrode which occur cross-linking reaction with CS for 35 min, following by washed with DI water to remove nonspecific binding GLD. Then, Ab (25 μL, 100μg/mL) was conjugated to the electrode and place in refrigerator at 4℃ for 24 h to full reaction. After that, the electrode was washed with PBS and dropped BSA (25 μL, 1%) at 37 ℃ for 0.5 h to block excess active sites. The electrode was rinsed with PBS and restored at 4 ℃ for the subsequent measurement of PEC signals. Finally, to prepare the

colorimetric detection, the TMB (20 mM, 20 μL), acetic acid (pH 4.5, 20 μL) and 10 μL PBS (pH 7.4, 0.1 M) were embedded in the color area.

The SEM and Raman data of $WO_3/BiVO_4$/Ab

To verified the immobilization of Ab on the prepared electrode, the SEM and Raman data of $WO_3/BiVO_4$/Ab shown in Fig. S7. As shown in Fig. S7A, after subsequent immobilization of Ab, cross-linked with glutaraldehyde and blocked aldehyde groups with BSA, the $WO_3/BiVO_4$ nanoflower surface turns obscure and seems being covered with a thin porous film. The clear change of morphological indicates that Ab has been successfully immobilized on the $WO_3/BiVO_4$ interface. As shown in Fig. S7B, the Raman peaks at 214, 272, 328, 366, 711, and 809 cm^{-1} are in agreement with the WO_3 and $BiVO_4$.[3] In curve B, the peak at 1370 cm^{-1} could be observed after introduction of Ab, and this peak is assigned to the stretching mode of COO^-, which indicates the successful incubation of Ab.[4]

The optimization of experimental conditions

To attain the best analytical performance of the PEC immunosensor, the PEC measurement conditions were carefully optimized, including the applied potential, the pH of electrolyte, the synthesis time of photoactive materials, and incubation time of AFP. All the optimization experiments were carried out by PEC signal in PBS containing 5 mM H_2O_2. From the Fig. S9A, the photocurrent ascended from 0.1 V to 0.4 V and then decreased at 0.5 V. The maximum photocurrent is about 14 μA at 0.4 V when the potential is within the range of 0-0.5 V. Therefore, the suitable potential of 0.4 V was chosen for detection of AFP. Besides, to obtain the optimal pH value of the PBS, we investigated the PEC signal in PBS (0.1 M) with different pH. As is shown in Fig. S9B, the peak photocurrent ascended with the increase of the pH of PBS, followed by the photocurrent drop off with the pH value increased. And the maximum photocurrent is about 13.8 μA at pH 6.5. As is shown in Fig S9C, the photocurrent is on the rise when the synthesis time is 1-5 h, but the signal has a declining trend when the synthesis time is 5 h. Therefore, the optimized synthesis time is 4 h. The optimal

incubation time of AFP indicated in Fig. S9D, the photocurrent decreased with the increasing incubation time of AFP and remained a steady value after 40 min. A longer incubation time did not enhance the PEC signal of the proposed biosensor. Therefore, to save detection time, 40 min was utilized for the reaction between Ab and target AFP (c_{AFP} = 0.1 ng mL^{-1}). The above results show that the optimum applied potential, pH, synthesis time, and incubation time are 0.4 V, 6.5, 4 h, and 40 min, respectively.

Colorimetric detection in clinical human serum samples

In order to quickly and easily detect the target of actual sample, we investigated colorimetric reaction in human serum (obtained from Shandong Tumor Hospital, China). At first, the TMB (20 mM, 20 μL), acetic acid (pH 4.5, 20 μL) and 10 μL PBS (pH 7.4, 0.1 M) were embedded in the color development area. At last, the lab-on-paper device was incubated with human serum (with ten-fold diluted). When 1 mL PBS containing 200 μL of H_2O_2 (5 mM) was introduced, we could see that the surface of paper chip turned blue. To obtain the more accurately illustrate the experimental results, we performed three times as shown in inset b of Fig. 5C. In parallel experiments, the lab-on-paper device could accurately realize the colorimetric detection of AFP in clinic human serum sample, indicating the proposed lab-on-paper device has acceptable accuracy.

Material	Detection range (ng mL^{-1})	LOD (ng mL^{-1})	Ref.
MIL-101(Cr)&CdSe QDs	0.1-300	0.082	[5]
Au/GaN	1-150	0.3	[6]
CuO NPs	0.05-500	0.038	[7]
Graded oxygen-doped CdS	0.2-100	0.0748	[8]
WO_3/$BiVO_4$ nanoflower	0.09-100	0.03	this work

Table S1 Comparison of other PEC-based AFP biosensors

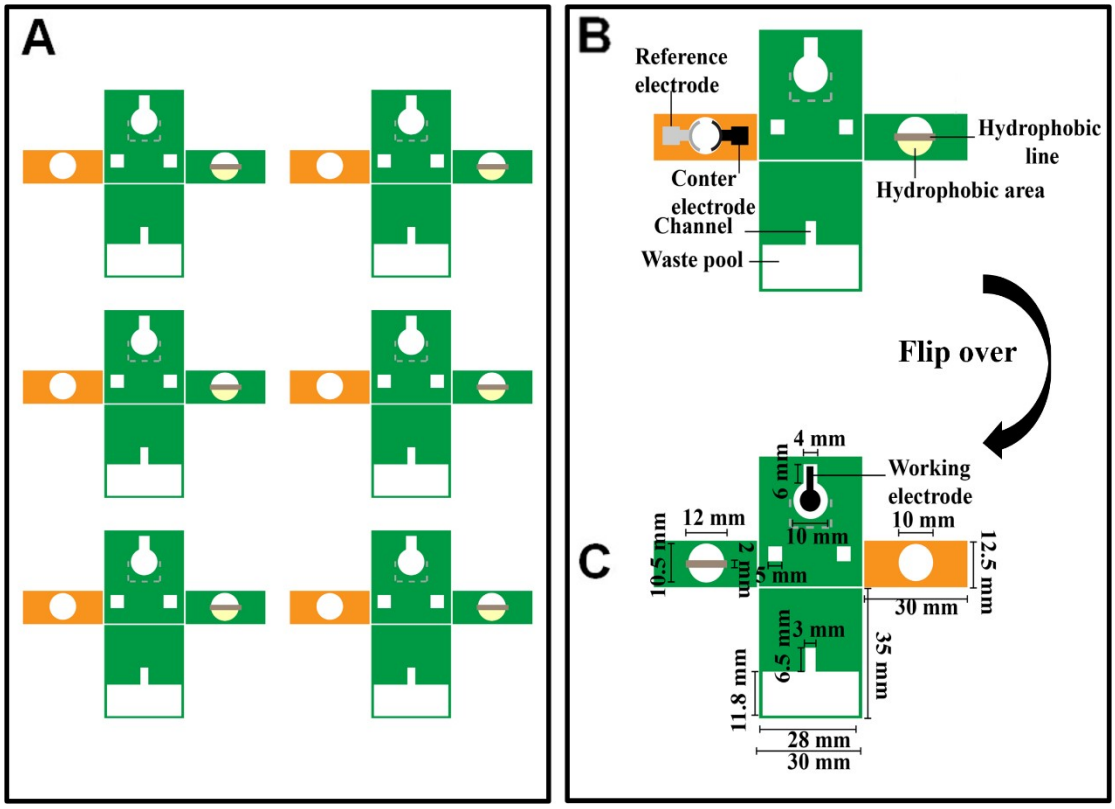

Fig. S1 (A-C) Wax pattern and physical schematic layout of lab-on-paper device based on 3D printing technology.

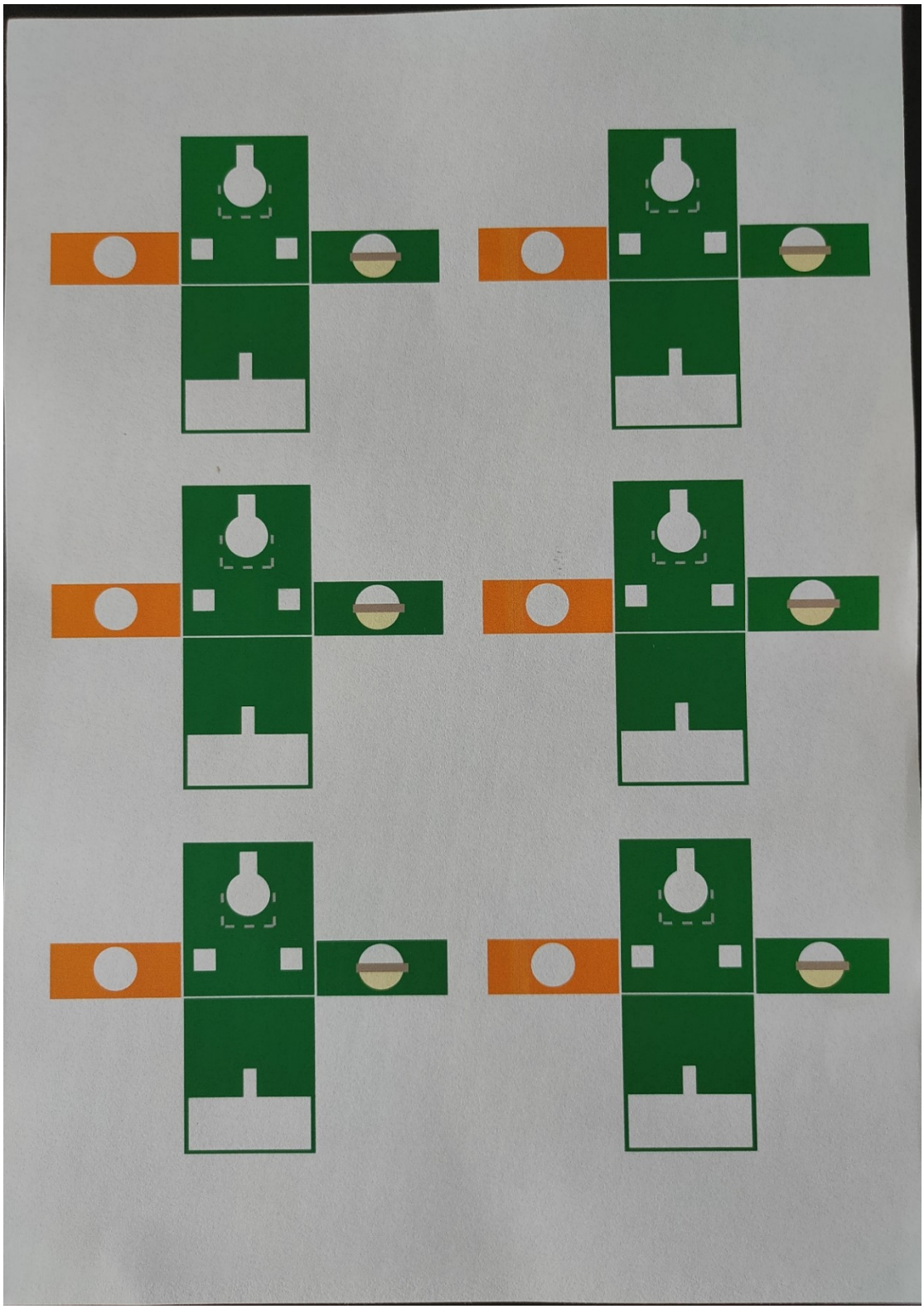

Fig. S2 Wax-patterns of lab-on-paper device on a paper sheet (A4) before baking.

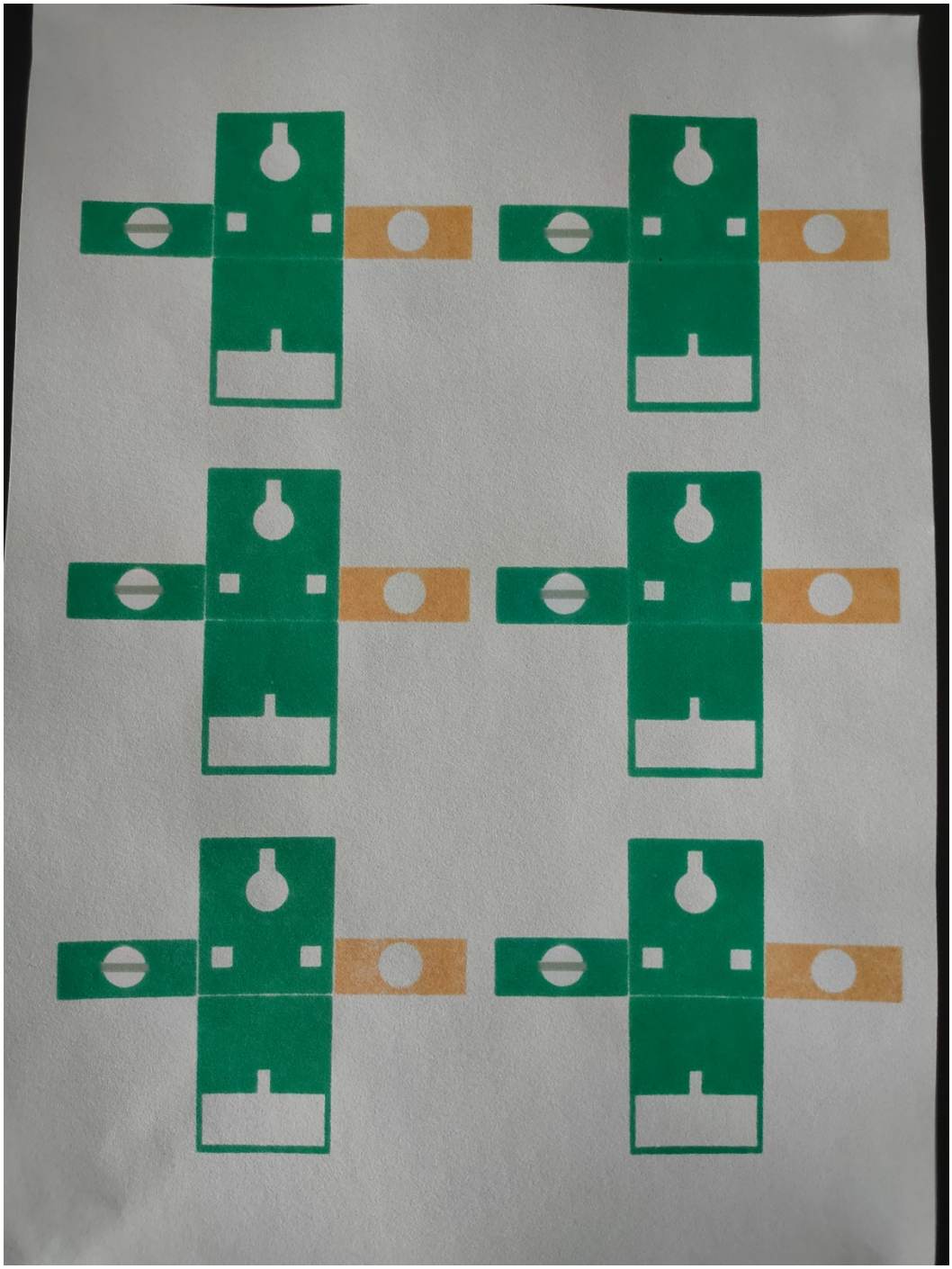

Fig. S3 Wax-patterns of lab-on-paper device on a paper sheet (A4) after baking (The reverse sides of Fig. S2).

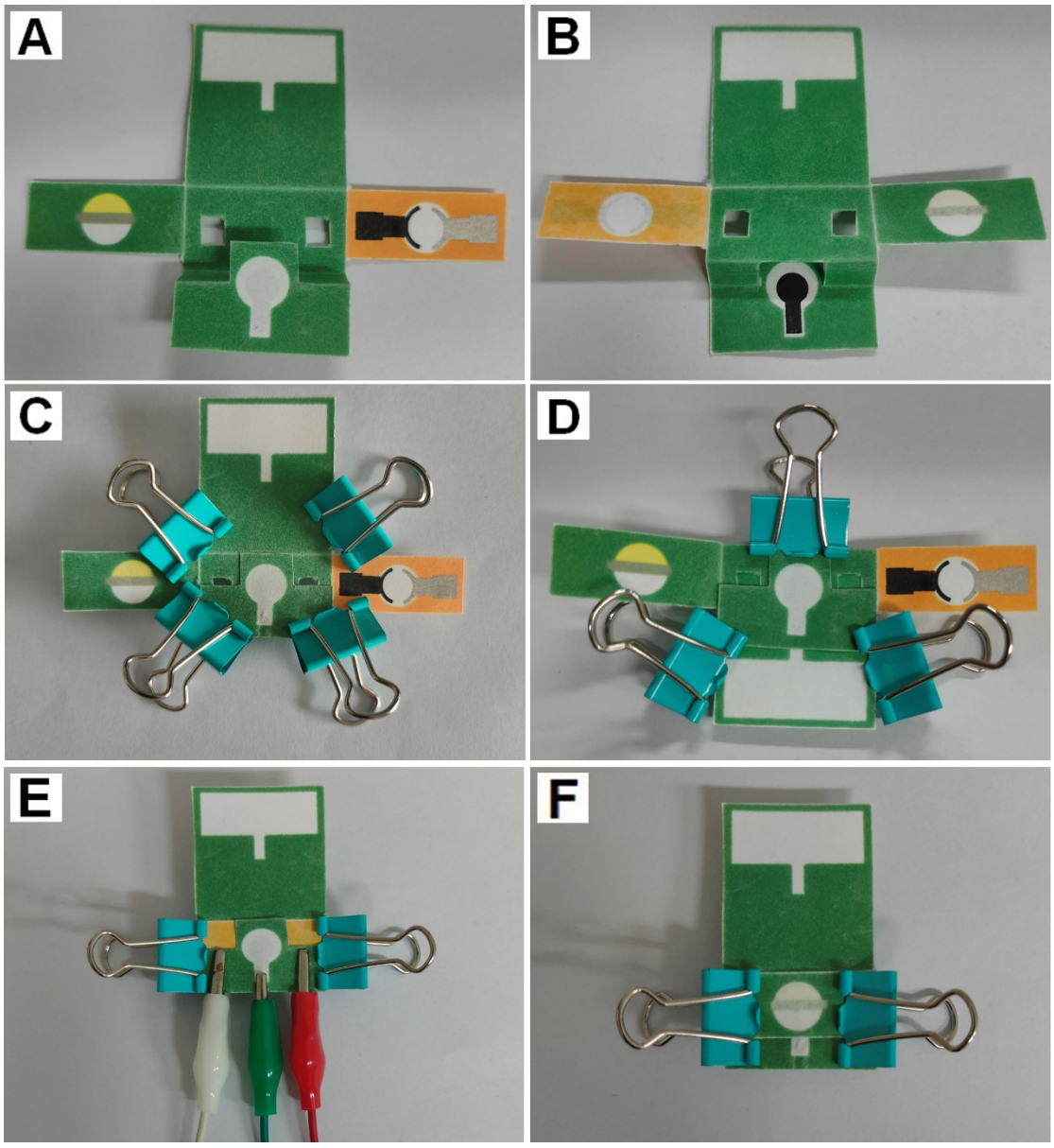

Fig. S4 The physical picture of (A), (B): Unfolded lab-on-paper device; (C): Lab-on-paper device folding during the process of electrode modification; (D): Lab-on-paper device folding during the process of cleaning; (E), (F): Lab-on-paper device folding during the process of PEC and colorimetric detection, respectively.

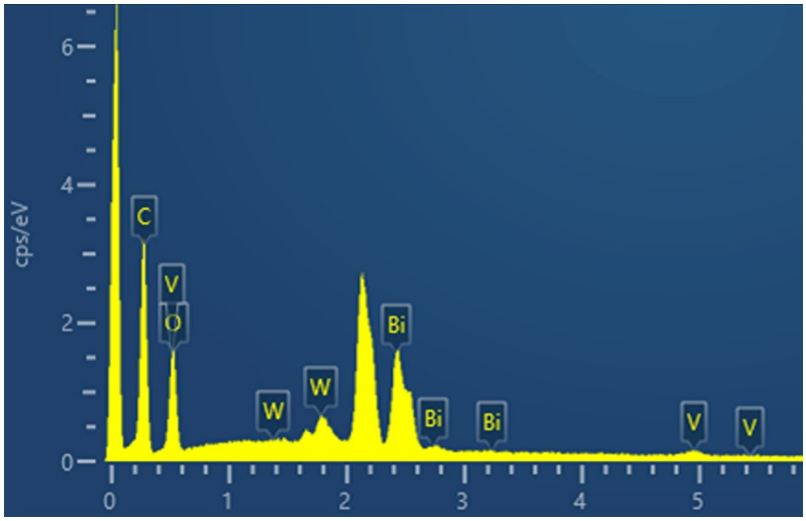

Fig. S5 EDS peaks of $WO_3/BiVO_4$.

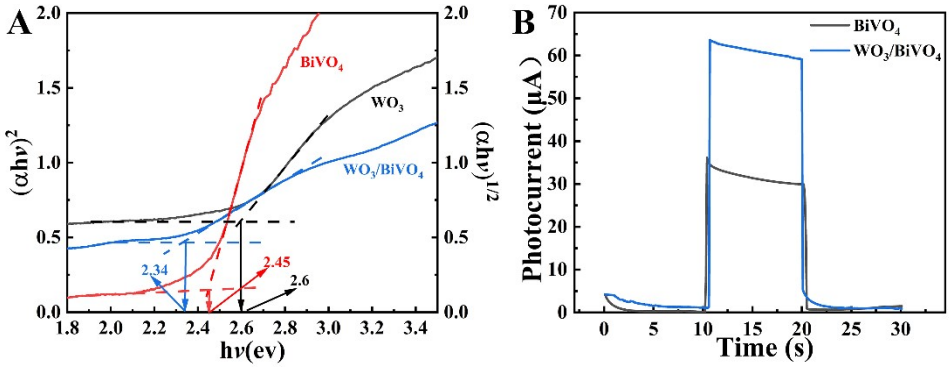

Fig. S6 (A) Tauc plots of WO_3, $BiVO_4$, $WO_3/BiVO_4$; (B) Photocurrent of $BiVO_4$ and $WO_3/BiVO_4$.

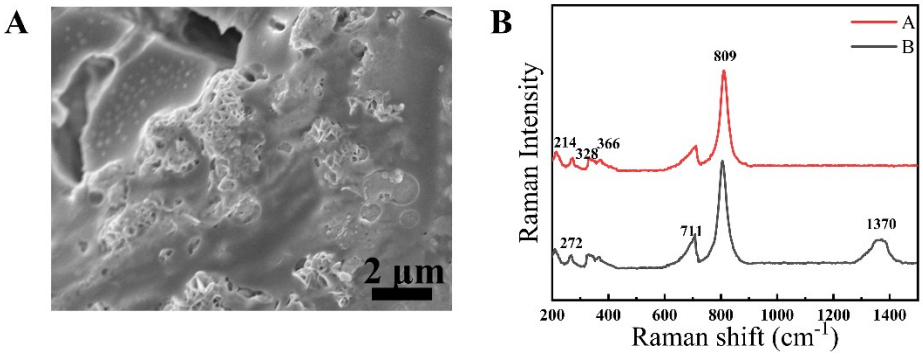

Fig. S7 (A) SEM of $WO_3/BiVO_4$/Ab; (B) Raman data of $WO_3/BiVO_4$/Ab.

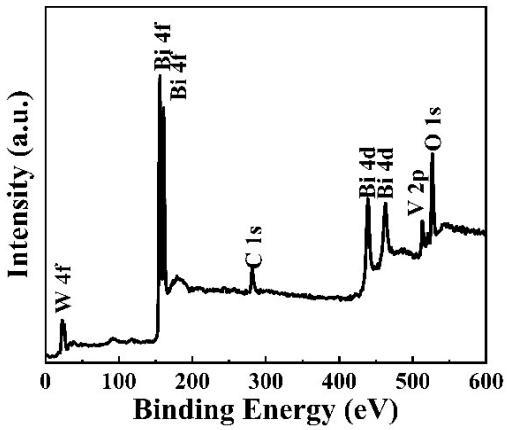

Fig. S8 XPS spectra of $WO_3/BiVO_4$ wide scan.

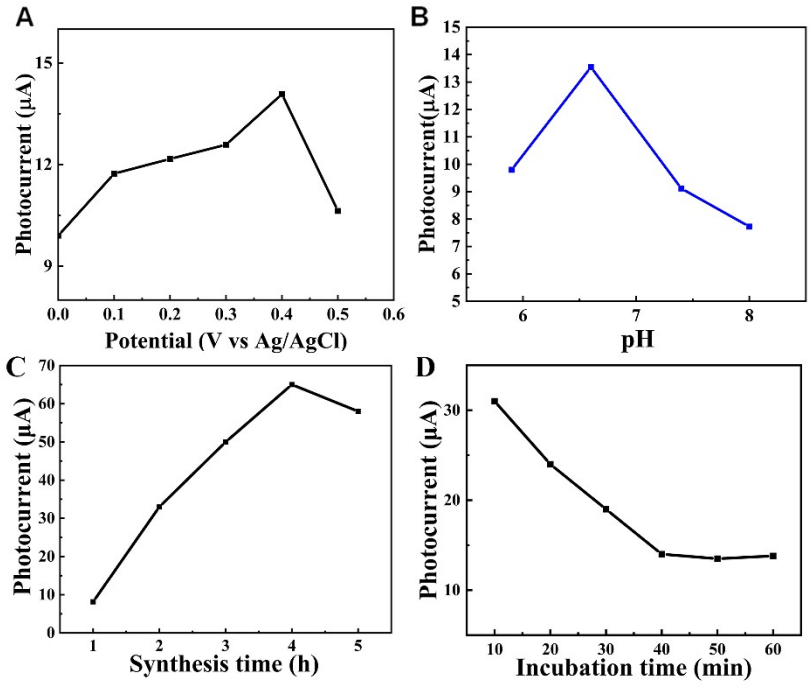

Fig. S9 Effect of (A) The potential of PEC measurement (c_{AFP} = 0.1 ng mL^{-1}); (B) The pH of buffer on photocurrent responses of biosensor (c_{AFP} = 0.1 ng mL^{-1}); (C) The photocurrent of different synthesis time of photoactive material; (D) The incubation time of AFP (c_{AFP} = 0.1 ng mL^{-1}).

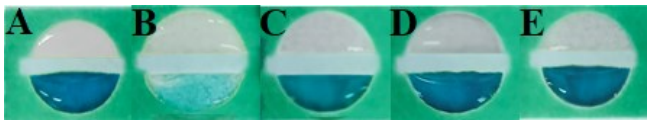

Fig. S10 Comparison of color development results of (A) blank; (B) AFP (c_{AFP} = 100 ng mL^{-1}); (C) CEA (c_{CEA} = 100 ng mL^{-1}); (D)PSA (c_{PSA} = 100 ng mL^{-1}); (E) H-lgG ($c_{H\text{-}lgG}$ = 100 ng mL^{-1}).

Reference

1. C. Zhou, K. Cui, Y. Liu, S. Hao, L. Zhang, S. Ge and J. Yu, *Anal. Chem.*, 2021, **93**, 5459-5467.
2. S. Phiankoh, P. Prajongtat, M. Chareonpanich and R. Munprom, *Energy Technol.*, 2020, **8**, 200147.
3. D. Coelho, J. P. R. S. Gaudêncio, S. A. Carminati, F. W. P. Ribeiro, A. F. Nogueira and L. H. Mascaro, *Chem. Eng. J.*, 2020, **399** 125836.
4. A. Zhu, X. Zhao, M. Cheng, L. Chen, Y. Wang, X. Zhang, Y. Zhang and X. Zhang, *ACS Appl. Mater. Interfaces*, 2019, **11**, 44617-44623.
5. Zhong. X, Zhang. M, Guo. L, Xie. Y, Luo. R, Chen. W, Cheng. F, Wang. L, *Biosens. Bioelectron.*, 2021, **189**, 113389.
6. Hu, D.; Cui, H.; Wang, X.; Luo, F.; Qiu, B.; Cai, W.; Huang, H.; Wang, J.; Lin, Z., *Anal. Chem.*, 2021, **93**, 7341-7347.
7. G. Wen and H. Ju, *Talanta*, 2015, **134**, 496-500.
8. Z. Yu, L. Huang, J. Chen, M. Li and D. Tang, *Sens. Actuators B,* 2021, **343**, 130136.